JOURNAL OF MATERIALS SCIENCE **38** (2003) 279–290

Decomposition of supersaturated solid solutions in Al–Cu–Mg–Si alloys

D. G. ESKIN
Netherlands Institute for Metals Research, Rotterdamseweg 137, 2628AL, Delft, The Netherlands
E-mail: d.eskine@tnw.tudelft.nl

The Al–Cu–Mg–Si alloying system is a base for a diverse group of commercial alloys which acquire their properties after quenching and aging. Therefore, the knowledge of the phase composition of hardening precipitates and the conditions under which they are formed is very important. Vast reference data were analyzed along with experimental results and calculations of phase equilibria. Different alloys were compared based on the composition of the supersaturated solid solution. It is shown that the phase composition of aging products in alloys with Mg : Si $>$ 1 agrees well with the equilibrium phase composition at a temperature of annealing. However, the sequence of precipitation in the alloys with Mg : Si $<$ 1 is more complicated. The hardening in these alloys occurs with precipitation of the β'' and θ' phases and their precursors. The former phase may contain copper and later transforms either to β' and β (Mg_2Si) or to Q phase depending on the amount of copper and annealing temperature.

1. Introduction

The Al–Cu–Mg–Si alloying system hosts several diverse groups of alloys such as wrought alloys of the 2XXX (with silicon as an impurity or an alloying element) and 6XXX series and foundry alloys of the 3XX series. Obviously, these alloys are located in different parts of the system and contain different ratios of constituent elements, i.e. copper, magnesium and silicon.

These alloys acquire their final mechanical properties after heat treatment including solution treatment, quenching (or cooling in air from the temperature of hot deformation or after casting) and aging to the maximum strength or to the maximum stability of properties. Evidently, these final properties are determined by the structure formed in these alloys upon heat treatment.* This structure can be described by the phase composition, morphology, distribution and size of precipitates formed during decomposition of the supersaturated solid solution.

The phase composition of these precipitates (and, therefore, their structure and, in most cases, morphology) is the most common topic of discussion in the modern literature. This problem has been studied now for half a century, each decade bringing new results and challenges. The precipitation in Al–Cu–Mg–Si alloys was studied by X-ray diffraction (1950–60's), transmission (TEM) and scanning (SEM) electron microscopy (1970–90's), differential scanning calorimetry (DSC) (1980–2000's), and high-resolution electron microscopy (HRTEM) (1990–2000's). Each stage of advances in examination techniques brought discoveries and confusions.

The uniqueness of the Al–Cu–Mg–Si system is that it is the only aluminium-based system where the quaternary phase Q (AlCuMgSi) formed by principal alloying elements exists and is in equilibrium with aluminium in the compositional ranges of commercial alloys. The other prominent feature of the system is that one of the elements, silicon, is actually not a metal but a semiconductor, which can make a difference in its interaction and phase formation with other, metallic constituents. This may be a factor responsible for the unique behavior of the β (Mg_2Si) phase upon precipitation and, eventually, for the controversial precipitation of the Q phase.

The precipitation of Si-free phases, S (Al_2CuMg) and θ (Al_2Cu), follows the pattern typical of other aluminum alloys with the initial zone and/or coherent stage of precipitation, then precipitation of a single semi-coherent modification of the equilibrium phase and, finally, the formation of the equilibrium phase.

Up to the 1990's the precipitation of the β phase in Al–Mg–Si and Al–Mg–Si-Cu alloys was supposed to comply with the usual picture. It was known that after the coherent monoclinic β'' phase, the semicoherent hexagonal β' phase precipitates, followed by the formation of the equilibrium cubic β phase. The application of high-resolution electron microscopy first to Al–Mg–Si and lately to Al–Mg–Si-Cu alloys showed that there is no unique β' phase but rather a series of intermediate phases (designated by tradition as β') with

*The properties are of course determined by other factors as well. Among these factors one can mention grain size and shape distribution, texture, macrosegregation, phases of solidification origin, intermetallics formed by transition metals, grain-boundary precipitates etc. However, with all these features being the same, the mechanical properties are mostly determined by the precipitation from the supersaturated solid solution.

TABLE I Chemical composition of examined alloys and the corresponding chemical composition of supersaturated solid solution (experimental/calculated[a])

	Alloy composition (wt%)			Supersaturated solid solution composition (wt%)			
Alloy no.	Cu	Mg	Si	Cu	Mg	Si	Mg : Si
1	4.0	1.6	0.15	3.9/3.95	1.6/1.4	0.15/0.06	10.7/23
2	4.1	1.0	0.15	4.1/4.1	0.9/0.99	0.10/0.13	9.0/7.6
3	4.1	0.8	0.30	4.1/4.1	0.7/0.76	0.27/0.27	2.6/2.8
4	4.5	0.45	0.25	4.2/3.95	0.40/0.43	0.25/0.22	1.6/1.9
5	4.1	0.30	0.40	4.1/3.9	0.30/0.29	0.40/0.38	0.75/0.76
6	4.2	1.8	0.25	4.2/4.02	1.2/1.4	0.10/0.08	12/17.5
7	4.6	1.5	0.5	4.4/4.32	0.90/0.92	0.16/0.17	5.6/5.4
8	4.5	1.2	0.63	3.8/4.18	0.60/0.76	0.30/0.28	2.0/2.7
9	4.5	1.5	0.13	4.1/4.35	1.25/1.34	0.10/0.09	12.5/14.9
10	4.5	1.2	0.61	4.0/4.23	0.8/0.75	0.25/0.28	3.2/2.7
11	5.0	0.30	5.0	4.2/3.98	0.25/0.30	0.70/0.87	0.36/0.34
12	–	0.05	0.70	–	0.05/–	0.70/–	0.07/–

[a]Calculated using Thermocalc^{TM} for 500°C.

different crystal structure and composition. This is a very prominent feature of Al–Mg–Si alloys the nature of which has not been explained yet.

The formation of the Q phase upon aging in Al–Cu–Mg–Si alloys is the most controversial subject also brought to life by HRTEM. Up to the late 1980's there was no evidence of precipitation of the quaternary phase in the wrought and foundry alloys during aging. Most TEM studies showed the precipitation of intermediate versions of the β, θ and Si phases in the compositional ranges of Q formation in the quaternary phase diagram. Particles of the equilibrium Q phase were observed in the structure of some alloys, but these particles were formed either during solidification or upon cooling from the temperature of solution treatment. Some authors claimed that they observed precipitation of the Q phase during aging, but only based on the fact that the alloy fell into the phase field with this phase in the equilibrium phase diagram. However, the use of the equilibrium phase diagram to predict the phase composition of precipitation products is obviously very dangerous. First of all, the decomposition of the supersaturated solid solution is a kinetic and non-equilibrium process. The precipitation occurs through several stages controlled by various factors such as diffusion and surface energy. In the case of multi-phase precipitation, as in Al–Cu–Mg–Si alloys, the sequence of phase precipitation and the gradual change of the solid-solution composition are of paramount importance. Secondly, and this is often forgotten, the chemical composition of the alloy determines the composition of the supersaturated solid solution but differs from it [1–4]. For many commercial alloys the amounts of alloying elements in the nominal composition and in the supersaturated solid solution differ by weight percents. And, finally, several phases and their modifications, which should not exist simultaneously, can coexist because of the kinetics of the process and different preferential sites of precipitation [5, 6].

At the same time, the equilibrium phase diagram can give a clue as to what the phase composition should be with respect to the equilibrium phases. Hence, the quaternary Q phase should form in the solid-solution compositions where this phase appears in the phase diagram, but not necessarily in the hardening stage of aging.

The HRTEM examinations of Al–Mg–Si alloys containing copper showed that under some temperature-time conditions a phase with the crystal structure and parameters of the equilibrium Q phase is formed. The surprise came when a similar phase was found in Al–Mg–Si alloys without copper. Since that time, several attempts were made to explain the observed phenomena. In our opinion, the explanation cannot be found without analyzing the phase composition in the entire compositional range of solid solutions in the Al–Cu–Mg–Si system.

In this paper, we will summarize the available experimental data in order to explain the precipitation in Al–Cu–Mg–Si alloys.

2. Experimental procedures

The experimental alloys listed in Table I were prepared from 99.99%[†] pure aluminum, 99.9% pure magnesium, Al–18% Si and Al–49% Cu master alloys. The alloys, except 9 and 10, were melted in an electric furnace and cast in a preheated mold with an inner cavity $\varnothing\, 20 \times 220$ mm. Alloys 9 and 10 were direct-chill cast to billets 134 mm in diameter. All alloys were solution treated at 500 ± 5°C for 8 h. Alloys 9 and 10 were then extruded at 400°C to plates 6×90 mm in cross-section. All the alloys were water quenched from 500°C and aged at 170°C with a delay between the quenching and the aging less then 10 min.

The chemical composition of the supersaturated solid solution was determined accurate to 5 rel.% using an X-ray microprobe analysis in a JSM-35CF scanning electron microscope equipped with a 4-crystal analyzer. The internal structure was examined in a JEM-2000EX transmission electron microscope. The phase identification was based on the calculation of selected-area electron diffraction patterns obtained in the same microscope.

In order to assess the composition of supersaturated solid solution for different alloys quenched from different temperatures, the calculations were performed

[†]Here and below wt% if not mentioned otherwise.

using a Thermocalc™ software. This software allows one to determine equilibrium concentration of the solid solution in a multicomponent alloy at any temperature and also gives information on the equilibrium phase composition at this temperature. The equilibrium chemical composition of the solid solution at a temperature of quenching was adopted as the chemical composition of the supersaturated solid solution. The comparison of the experimental and calculated chemical compositions in Table I shows good agreement between these series of values. The equilibrium phase composition was also determined for considered alloys at temperatures of aging (annealing).

3. Results and discussion

3.1. Phases existing in Al–Cu–Mg–Si alloys

The knowledge of phases which can precipitate in Al–Cu–Mg–Si alloys is necessary for further discussion. In this section, the information on the constituent phases is given with respect to the crystal structure, composition and conditions of formation.

Let us first consider the phases without silicon. The most examined phase is without any doubt Al_2Cu (θ). This phase starts precipitation with the formation of Guinier–Preston (GP) zones which consist of copper layer(s) in the {100} matrix planes, then the coherent θ'' phase and later the semi-coherent θ' phase precipitate, and finally the equilibrium Al_2Cu is formed. The coherent and semi-coherent modifications have a considerable hardening effect on Al–Cu alloys. Small additions of some elements are known to affect the precipitation of the θ phase [7, 8]. In the context of this paper, the effect of magnesium is the most interesting. Magnesium, being in solid solution, hampers the formation of the coherent phase and facilitates the precipitation of semi-coherent θ' alongside the refinement of its particles [9, 10]. This, generally, increases the hardening effect and the hardness level in Al–Cu alloys containing small additions of magnesium [9, 11]. The data on the crystal structure and other features of the Al_2Cu phase and its precursors are given in Table II. An indexed scheme of an observed electron diffraction pattern for the θ' phase is demonstrated in Fig. 1a.

Hence, small additions of magnesium favor the formation of the semi-coherent θ' phase. Further increase in the magnesium concentration in the supersaturated solid solution results in the formation of a new phase. This is the ternary Al_2CuMg phase the precipitation path of which is similar to that of the Al_2Cu phase: Guinier–Preston–Bagaryatsky (GPB) zones, coherent S″, semicoherent S′ and equilibrium S. The structure of all S-phase modifications are very close, therefore some authors consider them as a one structure differently distorted due to coherent or semicoherent junction with the matrix [14]. Sometimes, S″ denotes the ordered GPB2 zones. The clustering of Mg and Cu atoms at dislocations and then the precipitation of S′ phase at dislocation loops occur in the beginning of aging. At the final stage of hardening, GPB zones and the coherent S″ are formed in the matrix. Overaging results in the gradual formation of the incoherent S phase.

Table III gives some characteristics of the S phase. An indexed scheme of an observed electron diffraction pattern for the S′ phase is shown in Fig. 1b.

It is known that small additions of silicon to Al–Cu–Mg alloys cause the refinement of S precipitates. According to Hutchinson and Ringer [3] silicon is incorporated in GPB zones and facilitates their refinement and uniform distribution, and through that the refinement of hardening S precipitates.

The precipitation in Al–Mg–Si alloys and the corresponding hardening effect depends very much of the Mg : Si ratio. In the balanced alloy, the precipitation sequence is typical of the alloys considered above: zone formation, coherent needle-like β'' precipitates, semicoherent rod-shaped β' precipitates and formation of the equilibrium Mg_2Si phase. The excess of silicon (with respect to the stoichiometry of the Mg_2Si phase)

TABLE II Characteristics of Al_2Cu and its precursors

Phase	Crystal structure/morphology	Lattice parameters (nm)			Composition [Cu] (at.%)	Ref.
		a	*b*	*c*		
GPZ	–/Cu layer(s) in $\{100\}_{Al}$, disc	–	–	–	100	[8]
θ''	Tetragonal/plates	0.404	0.404	0.768	33	[13]
θ'	Body-centered tetragonal/plates	0.404	0.404	0.580	33	[12]
Al_2Cu	Body-centered tetragonal	0.6066	0.6066	0.4874	33	[13]

TABLE III Characteristics of the Al_2CuMg and its precursors

Phase	Crystal structure/morphology	Lattice parameters (nm)			Ref.
		a	*b*	*c*	
GPB	–/Cu, Mg segregates in $\{100\}_{Al}$, elipsoid discs elongated along $\langle 001\rangle_{Al}$	–	–	–	[6]
GPB2	Orthorhombic	0.405[a]	0.905	0.724	[13]
S″	Monoclinic/rods, laths	0.320	0.404	0.254 $\gamma = 91.3^\circ$	[6]
S′	Orthorhombic/laths at dislocation loops, corrugated packs in $\{210\}_{Al}$	0.404[a]	0.925	0.717	[13]
		0.404	0.89	0.76	[6]
Al_2CuMg	Orthorhombic/laths, rods	0.400	0.923	0.714	[13]

[a]Observed in this work, e.g. alloys 1, 2, 9 in Table I.

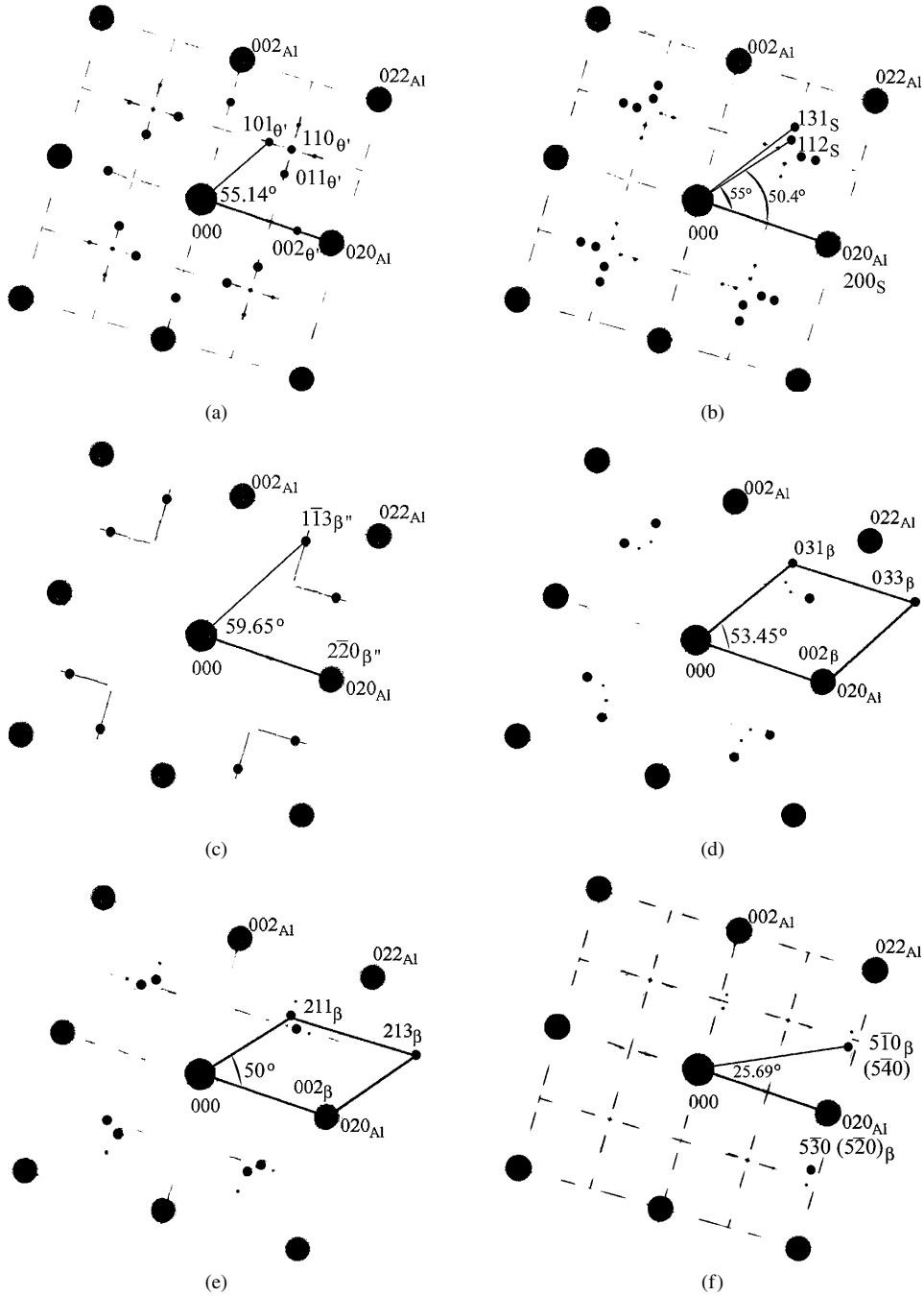

Figure 1 Indexed schemes of observed electron diffraction patterns: (a) θ' (e.g. alloys 3, 8, 10, 11 in Table I); (b) S′ (e.g. alloys 1, 2, 9 in Table I); (c) β'' (e.g. alloys 3–8, 10, 11 in Table I, aging 170°C, 20 h); (d, e) β'_C (alloy 11 in Table I, 250°C, 80 h); and (f) β'_C (alloy 5 in Table I, natural aging after quenching for 30 days and 170°C, 20 h).

can considerably change the kinetics of precipitation and the phase composition. As has been already mentioned the semicoherent phase has several modifications. These modifications are typical of Al–Mg–Si alloys with an excess of silicon [15].

The composition of metastable phases, i.e. Mg : Si ratio, is different from that of Mg_2Si (Mg : Si = 2 [at.%]). The Mg : Si ratio continuously increases in the series GPZ, β'', β', β [16], especially in alloys with an excess of silicon, Table IV. In other words, metastable phases are enriched in silicon. This means that the excess silicon must eventually form Si precipitates as it has been observed [5, 10, 17, 18]. Silicon precipitates have no hardening effect but their formation should always be taken into account when considering the composition of the supersaturated solid solution, sequence of precipitation and mass balance.

According to the most recent studies by Matsuda *et al*. [19], Edwards *et al*. [21] and Gupta *et al*. [27] the decomposition of the supersaturated solid solution in Al–Mg–Si alloys with an excess of silicon occurs as follows: clusters of Si and clusters of Mg → dissolution of Mg clusters → formation of Mg/Si clusters → "random" and "parallelogram"-type coherent needle-shaped precipitates (GPZ) → coherent needles β''; fine Si particles → semi-coherent rods β'; rods β'_B; rods β'_A; rods and laths of β'_C (B′), and plates and faceted particles of Si → plate- and cube-shaped β particles.

However, depending on the time-temperature conditions (isothermal annealing, temperature of annealing,

TABLE IV Characteristics of phases occurring in Al–Mg–Si alloys

Phase	Crystal structure/morphology	Lattice parameters (nm)			Mg : Si ratio (at.%) in balanced (excess Si) alloy	Ref.
		a	*b*	*c*		
GPZ	–/spherical	–	–	–	∼2 (∼1)	[20]
β''	Monoclinic/needles	0.616[a]	0.616	0.710 $\gamma = 82^\circ$		[13]
		0.714	0.658	0.405 $\gamma = 75^\circ$	1.74 (1.00)	[16]
		1.534	0.405	0.683 $\gamma = 106^\circ$	(1.2)	[21]
		1.516	0.405	0.674 $\gamma = 105.3^\circ$	(∼1)	[22]
β'	Hexagonal/needles, rods	0.705	–	0.405	0.44	[23]
β'_A	Hexagonal	0.405	–	0.67	(0.28, 0.2), 40 at.% Al	[24]
	Hexagonal	0.407	–	0.405	1.68	[25]
β'_C, B′, λ	Hexagonal/rods, laths	1.04[a]	–	0.405	(0.83, 1.1)	[21, 24, 26]
β'_B	Orthorhombic	0.684	0.793	0.405	(0.4), 40 at.% Al	[15, 24]
	Orthorhombic	0.672	0.787	0.405	1.75 (1.21)	[16]
β Mg_2Si	Cubic/rods, plates, cubes	0.639[a] or 0.6351	–	–	2.10 (2.13)	[13, 16]
Si	Cubic/faceted particles, plates	0.543[a]	–	–	–	[4, 5, 13]

[a]Observed in this work, e.g. alloys 5, 7, 8, 10, 11 in Table I.

TABLE V Composition and crystal structure of the Q phase and its precursors

Phase	Composition (wt%)			Lattice parameters (nm)		Ref.
	Cu	Mg	Si	*a*	*c*	
$Al_5Cu_2Mg_8Si_6$	20.3	31.1	27	1.032	0.405	[13, 30]
$Al_xCu_2Mg_{12-x}Si_7$	20.3	31.1	31.4	1.0393	0.4017	[31]
$Al_4CuMg_6Si_6$ (Q′) precursor	–	–	–	1.04	0.406	[19]
$Al_3Cu_2Mg_9Si_7$	–	–	–	–	–	[32]
$Al_5Cu_2Mg_8Si_6$	–	–	–	1.035	0.405	[33][a]
QC (precursor)	–	–	–	0.67	0.405	[33][a]
QP (precursor)	–	–	–	0.393	0.405	[33][a]
Q	20.6	32.6	30.2			[1]

[a]Precipitation in the matrix of Al–4% Cu–1% Mg–0.5% Ag/SiC composite.

precipitation upon heating etc.) the precipitation can go through this sequence or start at a certain stage. The decomposition starts directly with the formation of β'_C or β'_A particles at temperatures above 300°C, and the equilibrium β phase directly precipitates upon annealing above 400°C [5]. It should be noted that during high temperature annealing (at 300–350°C) the β' and equilibrium β phases may coexist for a long time, large incoherent precipitates with the structure of β' existing in the saturated solid solution [5, 15].

The coherent GP (Mg, Si) zones and β'' phase are efficient hardeners and participate in processes of natural and artificial aging. In the stage of softening they give place to various modifications of the β' phase which are considerably stable.

The maximum strength is achieved in alloys with an excess of silicon and in the stage of β'' precipitation. According to most references, there is no considerable hardening associated with the precipitation of β'-modifications [27–29].

The information on phases typical of Al–Mg–Si alloys is listed in Table IV. Fig. 1c–e present indexed schemes of some typical electron diffraction patterns observed in Al–Mg–Si and Al–Cu–Mg–Si alloys.

The effect of copper addition on Al–Mg–Si alloys depends on the amount of copper and on the Mg : Si ratio. This will be discussed in the following parts of this paper. Let us consider here the characteristics of the quaternary Q phase and its possible precursors. According to Mondolfo [13] this phase forms upon solidification and is in equilibrium with aluminum under the following conditions: Mg : Si < 1.73 (wt%), [Mg] > 2 [Cu], and [Cu] > 1 wt%. Depending on the ratio between copper, magnesium and silicon, this phase can coexist with Al_2Cu, Mg_2Si and Si. The equilibrium Q phase has a hexagonal crystal structure with lattice parameters and composition given in Table V according to various sources.

It should be particularly noted that the β'_C phase in ternary Al–Mg–Si alloys with an excess of silicon and the Q phase observed in quaternary Al–Mg–Si-Cu alloys have the same structure and differ only in the composition, the Q phase containing copper [19, 29, 34]. Most of the authors report that the Q phase precipitates in Al–Cu–Mg–Si alloys in the form of laths whereas the β'_C phase forms rods. Obviously, the morphology is not a sufficient argument for the attestation of a new phase. There is strong evidence that copper dissolves in the β'' phase which then evolves either to β or to Q phase depending on the alloy composition and conditions of precipitation [29, 35]. Wolverton [32] suggests that the composition of Q might be temperature-dependent, because the phase exists in a compositional off-stoichiometric range. It should be noted that there is no strong support for the hardening ability of the Q phase or its precursors.

There are other phases which are sometimes observed in Al–Cu–Mg–Si alloys. They are worth mentioning because their appearance confirms a highly nonequilibrium character of precipitation in the alloys of this system. The cubic σ ($Al_5Cu_6Mg_2$) phase with the lattice parameter $a = 0.831$ nm was observed to precipitate in Al–Cu–Mg alloys containing silicon (Cu : Mg $\sim$ 2–3) [36, 37]. This phase cannot be in equilibrium with the aluminium solid solution [13]. However silicon additions to Al–Cu–Mg alloys decrease the density of dislocation loops—the preferential sites for S′ precipitation. As a consequence the compound next in the phase diagram forms homogeneously in the matrix, providing the annealing temperature in sufficient—above 200°C. The shape of these precipitates is cubic [36, 37]. This phase competes in precipitation, and often coexists, with S′ and θ'. The former phase prevails when dislocation loops are present, the latter, when the local concentration of magnesium is not sufficient [37]. Hirosawa *et al*. [7] remark on the similarity between Si and Ag effects on the precipitation in Al–Cu–Mg alloys with respect to their interaction with Mg, Cu and vacancies. This is confirmed by the observation of the Ω phase in a 2024 alloy containing no silver but 0.5% Si [38]. This phase, which is a modification of the Al_2Cu phase, is usually observed in Al–Cu–Mg alloys with silver [8]. The composition of Ω is the same as that of Al_2Cu phase and the structure, either orthorhombic or tetragonal, is very close to that of the equilibrium Al_2Cu phase. After prolonged annealing the Ω phase is replaced by Al_2Cu, which confirms that the former is the metastable modification of the latter. The main difference between Ω and θ' is the morphology (hexagonal platelets and elongated plates, respectively) and the habitus plane ({111} and {100}, respectively).

3.2. Phase composition of precipitates in Al–Cu–Mg–Si alloys with respect to the composition of the supersaturated solid solution

There have been several attempts to interpret the experimental results on precipitating phases in Al–Cu–Mg–Si alloys using the phase diagram, the chemical composition of the supersaturated solid solution and accounting for the change in this composition during precipitation.

The effect of small additions of silicon on the phase composition after precipitation in Al–Cu–Mg alloys was well explained using the isothermal, low-temperature cross-section of the equilibrium Al–Cu–Mg phase diagram and the amount of magnesium removed from the supersaturated solid solution by the precipitated Mg_2Si phase [3, 11].

Chakrabarti *et al*. [39] made an attempt to generalize the phase composition of precipitates in Al–Cu–Mg–Si alloys by putting the chemical compositions of alloys on the portion of the equilibrium phase diagram with Q-containing phase fields and comparing the equilibrium phase composition with the experimental data on the metastable precipitates. Although their paper contained a very useful collection of data, the use of chemical compositions of alloys and the equilibrium phase diagram did not provide a good match with the experimental data. However, it has been shown that Q phase could be observed after precipitation in the compositional range where this phase should be present according to the equilibrium phase diagram.

Eskin *et al*. [4, 10] measured the composition of the supersaturated solid solution in examined alloys by X-ray microprobe analysis and then put these data on the diagram along with the experimentally determined phase composition after peak hardness aging at 170°C. To the best of our knowledge, this have been the only attempt to cover the entire range of supersaturated solid solutions in Al–Cu–Mg–Si alloys containing 4% Cu. It was shown that the phase composition after decomposition in the alloys with excess magnesium (Mg : Si > 1.73 [wt%]) agreed fairly well with the equilibrium phase composition. However, the metastable phase regions for the alloys with excess silicon (Mg : Si < 1.73) contained β'' instead of Q, the latter phase being present in the equilibrium phase diagram. It should be particularly stressed that these phase compositions reflected the peak hardness condition achieved at 170°C.

In the present paper, the available information on the phases formed upon decomposition of supersaturated solid solution is analyzed with respect to the initial chemical composition of the supersaturated solid solution and to the Mg : Si ratio at different levels of copper concentration. The reference data used in this study are listed in Tables VI and VII alongside the calculated chemical composition of the aluminum solid solution at a temperature of quenching and the equilibrium phase composition of alloys at a temperature of aging (annealing). Note that in many alloys the difference between the experimentally observed phases and the equilibrium phase composition is striking.

The results of the analysis are summarized in a form of diagrams, Fig. 2. Each diagram covers some, rather arbitrarily chosen, range of copper concentrations. The points in the diagrams represent the compositions of the initial supersaturated solid solutions in alloys listed in Tables I, VI and VII. By no means, these diagrams reflect the metastable equilibrium. However, this technique allows us to compare different alloys processed by different heat-treatment routine.

Fig. 2a shows a diagram for alloys containing up to 0.25% Cu, which reflects wrought alloys of 6XXX series like 6022, 6016, 6009, 6061 and foundry Al–Si–Mg alloys. Obviously, the main precipitating phase is β in its metastable modifications. Copper may dissolve in the β' phase. The hexagonal phase with lattice parameters $a = 1.04$ nm and $c = 0.405$ nm (β'_C) is observed in alloys with Mg : Si < 1.2 (in wt%). An electron diffraction pattern of this phase is indexed in Fig. 1d and e. In the alloys with an excess of silicon (Mg : Si < 1), Si forms its own particles. According to the equilibrium phase diagram [40] and our calculations (Tables VI and VII), the Q phase is present alongside β and Si in alloys with Mg : Si < 1.73 even at very small amounts of copper. However, there is no reliable evidence of its precipitation upon decomposition of the

TABLE VI Data on the chemical composition of alloys referred to in this study

No.	Alloy composition (wt%)			Composition of the Al solid solution (s.s) (calculated[a]/reported) (wt%)			Mg : Si in s.s.	Ref.
	Cu	Mg	Si	Cu	Mg	Si		
1	–	0.63	0.37	–	0.63	0.37	1.7	[19]
2	–	0.93	0.77	–	0.93	0.77	1.21	[19]
3	–	0.63	0.35	–	0.63	0.35	1.8	[16]
4	–	0.64	0.81	–	0.64	0.81	0.9	[16]
5	–	0.68	0.89	–	0.68	0.89	0.76	[5]
6	–	0.9	0.9	–	0.74	0.81	0.91	[5]
7	0.01	1.1	1	0.01	0.75	0.8	0.94	[26]
8	0.07	0.58	1.28	0.06	0.57	1.28	0.45	[54]
9	0.18	0.8	0.79	0.18	0.80	0.79	1.01	[21]
10	0.25	1.0	0.9	0.25	0.66	0.7	0.94	[35]
11	0.39	0.61	1.22	0.38	0.6	1.22	0.49	[29]
12	0.5	0.63	0.37	0.5	0.63	0.37	1.7	[19]
13	0.6	0.4	7.0	0.6	0.4	0.93	0.43	[18]
14	0.6	0.6	0.8	0.6	0.53	0.76	0.70	[45]
15	0.69	0.54	0.55	0.69	0.53	0.55	0.96	[46]
16	0.68	1.35	0.82	0.68	1.03	0.64	1.61	[47]
17	0.75	0.75	0.63	0.74	0.71	0.6	1.18	[41]
18	0.75	0.75	0.63	0.74	0.71	0.6	1.18	[48]
19	0.91	0.55	1.26	0.91	0.55	1.26	0.44	[54]
20	1.04	0.99	12	1.06/0.46	0.39/0.3	0.8/1.0	0.49	[42]
21	1.01	0.78	12	1.07/0.97	0.4/0.48	0.81/1	0.49	[49]
22	1.52	0.74	0.23	1.52/1.52	0.73/0.74	0.22/0.23	3.32	[1, 50]
23	1.51	0.75	0.49	1.51/1.45	0.74/0.63	0.48/0.39	1.54	[1, 50]
24	1.54	0.75	0.76	1.53/1.37	0.65/0.44	0.71/0.50	0.92	[1, 50]
25	1.52	0.77	1.03	1.52/1.16	0.56/0.05	0.91/0.44	0.62	[1, 50]
26	2.5	1.5	0.1–0.25	2.5/2.5	1.4/1.2–1.0	0.13/0.1–0.25	10.8	[3]
27	2.5	1.5	0.5	2.5/2.5	1.04/0.9	0.24/0.5	4.3	[3]
28	3.0	0.1	0.6	2.97	0.09	0.6	0.15	[33][b]
29	3	0.39	7.1	2.41	0.29	1.17	0.25	[55]
30	3.63	1.67	0.5	3.58	1.17	0.195	6.0	[36]
31	4	1	0.7–1.2	3.72	0.49	0.51 (at 0.95% Si)	0.96	[33][b]
32	4.38–4.53	0.3–0.34	0.5	4.5	0.29	0.48	0.6	[51][b]
33	4	0.3	0.1	4.0	0.29	0.08	3.63	[44]
34	4	0.3	0.2–0.7	4.0	0.29	0.48 (at 0.5% Si)	0.6	[44]
35	4	0.3	1.2	4.0	0.29	0.99	0.29	[44]
36	4.3	0.53	0.87	4.21/4.0	0.38/0.4	0.73/0.7	0.52	[43]
37	4.57	0.42	0.66	4.57	0.4	0.64	0.63	[52]
38	4.3	0.85	0.94	4.02	0.4	0.55	0.73	[53]
39	4.3	2.0	0.35	3.11	1.48	0.15	9.87	[37]

[a]Calculated using Thermocalc^{TM} for equilibrium composition of the solid solution at a temperature of homogenization.
[b]Alloys with Ag.

supersaturated solid solution, in particular on its contribution to precipitation hardening.

With the increase of copper concentration in an alloy to 0.5–0.8% (alloys like 6013, 6111, 2008) the situation essentially remains the same, Fig. 2b. The precipitating phase is mainly β in its modifications. However, some authors report Q′ alongside β [19, 41]. This observed phase has the structure and morphology identical to the β'_C phase, but contains copper. The equilibrium phase composition in the considered compositional range changes on decreasing the Mg : Si ratio from $Mg_2Si + Al_2Cu + Q$ to $Q + Al_2Cu + Si$.

Further increase of copper content in an alloy makes the precipitation pattern more complex, Fig. 2c. Depending on the Mg : Si ratio the main hardening phase is S′ or GPB (Mg : Si > 3), θ' (0.5 < Mg : Si < 2) or β'' (Mg : Si < 0.5). The latter phase may contain copper [29]. In the alloys containing Mg : Si < 2 the equilibrium Q phase forms during solidification or sometimes is observed upon long annealing at high temperatures. Silicon forms its own particles at Mg : Si < 1.

Finally Fig. 2d shows the phase composition of alloys containing 2.5–4.5% Cu (alloys like 2036, 2017, 2024, 2014). Apart from the appearance of σ phase, the phase composition of precipitation products is in good agreement with the equilibrium phase composition for alloys with Mg : Si > 1, even at the hardening stage of precipitation. The θ' phase precipitates in all alloys containing Mg : Si < 8 (Figs 1a and 3b); S′ phase is present at Mg : Si > 3 (Figs 1b and 3c); the β'' (β') is formed at 1 < Mg : Si < 8 (Figs 1c and 3b). However, in the alloys with an excess of silicon (Mg : Si < 1) where the Q phase is present according to the equilibrium phase diagram (Tables VI and VII) there is a controversy. At the hardening stage of precipitation, the main phases here are θ' and β''. Our results showed no evidence of precipitating β' or Q phases upon aging at 170°C. However, we observed some rather unusual reflections in alloys with an excess of silicon aged at 170°C after natural aging for 30 days (Figs 1f and 3d). Previously [4] we ascribed these reflections to the S″ phase (orthorhombic) with the following orientation

TABLE VII Data on the phase composition of alloys referred to in this study

No. in Table VI	Heat treatment: Homogenization/Annealing (°C)	Phase composition after annealing experimental/equilibrium[a]	Ref.
1	575/250	β'/Mg_2Si	[19]
2	575/250	β'', β'_C/Mg_2Si	[19]
3	550/175; 250; 350	β'', β'/Mg_2Si	[16]
4	550/175; 250; 350	β'', β', β, Si/Mg_2Si, Si	[16]
5	550/300	β'_C; β; Si/Mg_2Si, Si	[5]
6	550/350	β'_A; β; Si/Mg_2Si, Si	[5]
7	550/185	M (Q)/Mg_2Si, Si, Q (negl. amount)	[26]
8	560 + NA/DSC	β'', $\beta' + Q$, $\beta + Si/Si$, Mg_2Si, Q (at 200°C)	[54]
9	DSC	β'', B′, β', β/Q, Mg_2Si, Si (at 200°C)	[21]
10	535/300	β', β'_C (with Cu), β/Mg_2Si, Q, Si	[35]
11	550/175	β'' (with Cu)/Q, Si, Mg_2Si (small amount)	[29]
12	575/250	Random type, β', Q′/Mg_2Si, Al_2Cu, Q	[19]
13	?[b]/170	β'', Si/Si, Q, Al_2Cu	[18]
14	?[b]/200	β'/Q, Si, Al_2Cu	[45]
15	560/175	β'', $\beta' + Q$/Q, Al_2Cu, Si (small amount)	[46]
16	568/175	β'/Mg_2Si, Al_2Cu, Q	[47]
17	535/180	β'', Q′/Q, Al_2Cu, Mg_2Si (small amount)	[41]
18	535/315	Q (grain bound., disloc.)/Q	[48]
19	560 + NA/DSC	β'', Q′, Q + Si/Q, Al_2Cu, Si	[54]
20	?[c]/DSC	GP, S′, Si/Si, Q, Al_2Cu	[42]
21	?[c]/DSC	β', Si/Si, Q, Al_2Cu	[49]
22	530/190	GPB, S′/Al_2CuMg, Al_2Cu, Mg_2Si	[1, 50]
23	530/190	GP, θ', insoluble Q/Al_2Cu, Mg_2Si, Q	[1, 50]
24	530/190	GP, θ', insoluble Q/Q, Al_2Cu, Si	[1, 50]
25	530/190	GP, θ', insoluble Q/Q, Al_2Cu, Si	[1, 50]
26	525/200	GPB/Mg_2Si, Al_2CuMg	[3]
27	525/200	GPB (with Si), S, θ', σ/Mg_2Si, Al_2Cu, Al_2CuMg	[3]
28	500 + NA/170	θ', QP, Si/Al_2Cu, Si, Q	[33][d]
29	540/175	θ', β'', (L) B′, Si/Si, Al_2Cu, Q	[55]
30	525/200–265	σ, S′, θ'/Al_2CuMg, Al_2Cu, Mg_2Si	[36]
31	500 + NA/170	θ', θ'on QC, QP in matrix/Al_2Cu, Q, Si	[33][d]
32	530 + NA/190	θ', S′/Al_2Cu, Mg_2Si, Al_2CuMg	[51][d]
33	520/200	θ', S′ (?)/Al_2Cu, Mg_2Si, Al_2CuMg	[44]
34	520/200	θ', Q′ (overaged)/Al_2Cu, Q, Si	[44]
35	520/200	θ', Q (few), Si/Al_2Cu, Q, Si	[44]
36	505 + NA/150	θ', λ'(Q′ ?)/Al_2Cu, Q, Si	[43]
37	520/185	GP, λ', θ'/Al_2Cu, Q, Si	[52]
38	500 + NA/DSC	θ', S′/Al_2Cu, Q, Si (at 200°C)	[53]
39	530/190	σ, θ', β', S′/Al_2CuMg, Al_2Cu, Mg_2Si	[37]

[a]Calculated using Thermocalc™ for the equilibrium phase composition at a temperature of aging/annealing. Phases are shown in descending order with respect to their weight fraction at this temperature.
[b]520°C for calculation.
[c]500°C for calculation.
[d]Alloys with Ag.

relationship: $(\bar{1}21)_p \parallel (001)_{Al}$; $\langle 1\,\bar{1}3\rangle_p \parallel \langle 100\rangle_{Al}$. The reason was that there is a possibility that GPB zones may form at room temperature and then, being quite stable, act as nuclei for an S-based phase. Smith *et al.* [42] also observed these reflections in a 2124 alloy and interpreted them as belonging to the S phase. However, some authors observed precipitation of a phase containing copper and having the lattice parameters as the equilibrium Q phase (which are the same as those of β'_C) in the alloys containing Mg : Si < 1 [33, 43, 44]. Modifications of the (AlCuMgSi) phase were found in silver-containing alloys [33, 34]. The reflections shown in Figs 1f and 3d and typical of the alloys artificially aged after a delay between the aging and the quenching can be interpreted as belonging to the β'_C (Q) phase with the following orientation relationship: $(5\,\bar{3}0)_p$ or $(5\,\bar{2}0)_p \parallel (002)_{Al}$; $\langle 001\rangle_p \parallel \langle 100\rangle_{Al}$. It is noteworthy that there were no particles found associated with these reflections. That can attest to the fact that the amount of the phase giving these reflections is very small. After overaging (250°C, 80 h), the β'_C (Q) phase with two orientation relationships (Fig. 1d and e, 3a): $(001)_p \parallel (001)_{Al}$; $\langle\bar{1}20\rangle_p \parallel \langle 100\rangle_{Al}$ and $(001)_p \parallel (001)_{Al}$; $\langle 100\rangle_p \parallel \langle 100\rangle_{Al}$ can be clearly distinguished by electron diffraction patterns alongside the θ' phase. It should be also mentioned that Si forms its own particles in the alloys with an excess of silicon. However, these particles proper and, in particular, electron-diffraction reflections from these particles are hardly visible until the particles grow considerably.

3.3. Hardening with respect to the phase composition

Experimental results obtained in this study show that in the alloys with 4% Cu hardening at 170°C occurs, depending on the Mg : Si ratio, through precipitation of the following phases: S′, θ', and β'' phases, either individually or in combination. Best hardening ability is demonstrated by alloys with the $\theta' + \beta''$

hardening combination [4]. The compositions of the supersaturated solid solutions for these alloys are listed in Table I and the corresponding phase compositions of aging products are shown in Fig. 2d.

An interesting feature of wrought 2024-type alloys (alloys 9 and 10 in Table I) is that the addition of Si in the stoichiometric ratio with Mg causes a change of hardening phases from S′ to $\theta' + \beta'' + S'$ with the potential for improved mechanical properties [4, 10, 11].

Hutchinson and Ringer [3] also observed that addition of up to 0.5% Si to an Al–2.5% Cu–1.5% Mg alloy resulted in the shift of the phase composition after aging from S′ to $S' + \theta' + Mg_2Si$ and corresponding increase in the hardening effect.

Gao *et al*. [44] reported that the phase composition after aging at 200°C of an Al–4% Cu–0.3% Mg alloy changes from $S' + \theta'$ to $\theta' +$ {rod/lath-shaped precipitates} + Si on increasing the concentration of

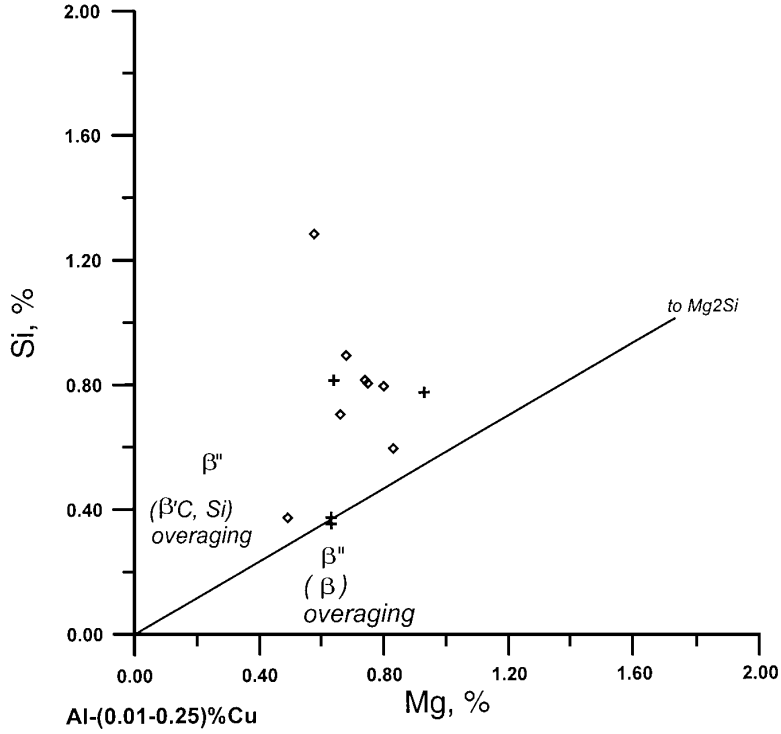

(a)

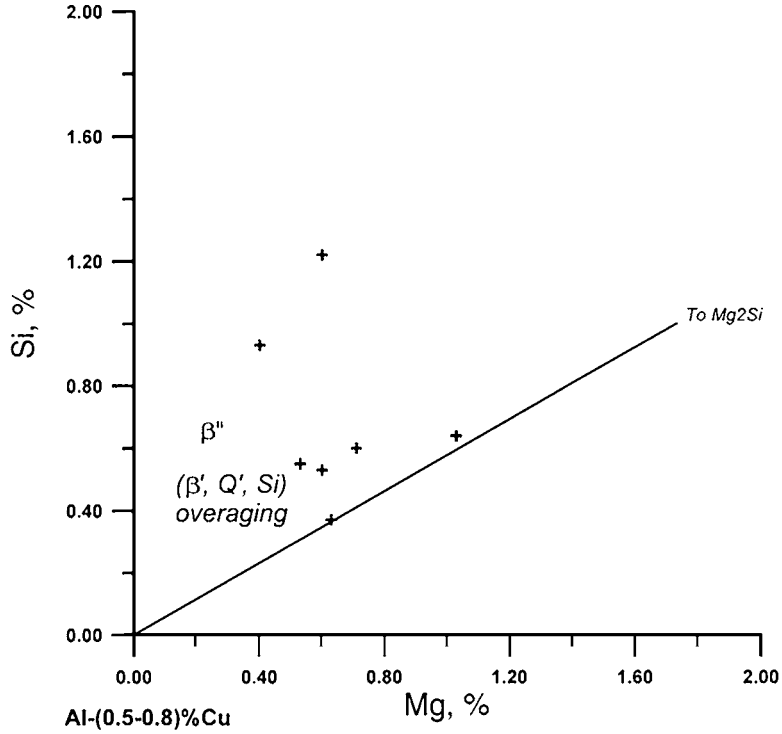

(b)

Figure 2 Experimentally observed phase compositions after decomposition of supersaturated solid solutions for alloys with (a) 0–0.25% Cu; (b) 0.5–0.8% Cu; (c) 0.9–2.5% Cu; and (d) 2.5–4.5% Cu. ● – own data [4, this study]; + – ref. data, peak hardness; ◊, ♦ – ref. data, overaged alloys or DSC. Phase symbols denote the phase composition at the peak hardness, if otherwise is not noted. (*Continued*.)

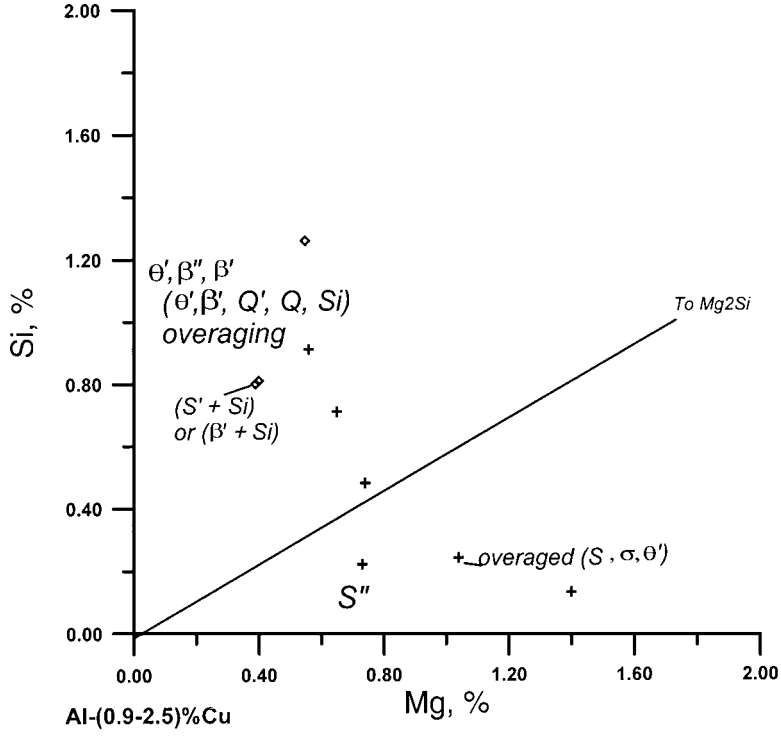

(c)

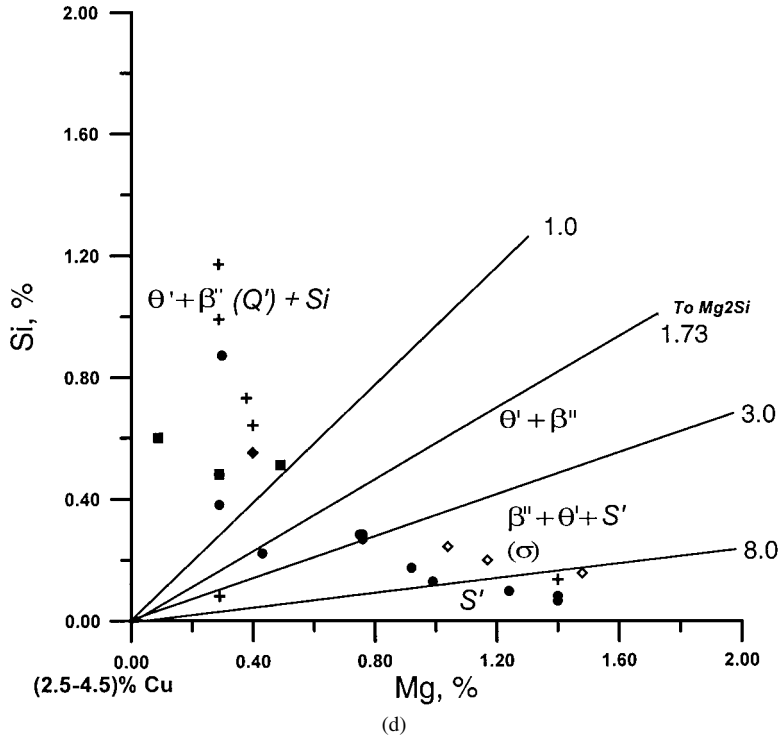

(d)

Figure 2 (*Continued*).

silicon from 0 to 1.2%. The rod/lath-shaped precipitates were identified as Q phase in the overaging stage of precipitation.

The most arguable phase composition is that of alloys with an excess of silicon where the Q phase or its precursors were observed at various stages of annealing. However, there is hardly any evidence of its precipitation at the hardening stage of aging at temperatures below 200°C.

Reference data show that the hardening upon aging of Al–Cu–Mg–Si alloys with less that 2–4 wt% Cu also occurs due to the precipitation of the β'' phase. Murayama *et al*. [29] reported that only β'' containing copper was observed upon aging of an Al–0.39% Cu–0.61% Mg–1.22% Si alloys at 175°C. The Q′ phase was observed only after annealing at 280–300°C. Perovic *et al*. [41] found both β'' and Q upon aging at 180°C, the latter phase substituting the former on increasing aging time. Miao and Laughlin [54] concluded that the β'' phase is responsible for age hardening at 175°C in an Al–0.91% Cu–0.55% Mg–1.26% Si alloy, this phase containing copper and later transforming to Q′.

A peculiar group of alloys containing silicon in excess to Mg_2Si is formed by casting Al–Si alloys or silumins. According to the phase diagram [40], the

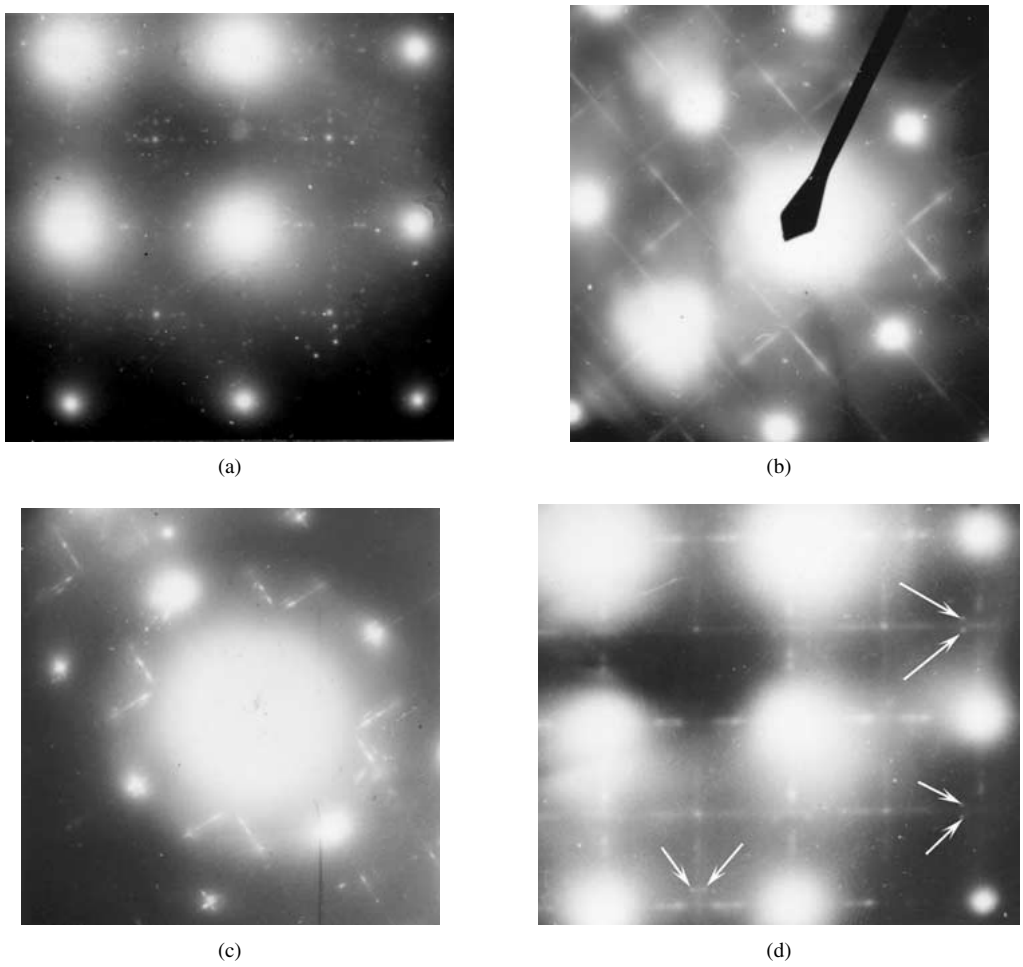

Figure 3 Experimental electron diffraction patterns: (a) alloy 11 in Table I, 250°C, 80 h; (b) alloy 11 in Table I, 170°C, 20 h; (c) alloy 9 in Table I, 170°C, 20 h; and (d) alloy 5 in Table I, 170°C, 20 h after 30-days natural aging.

supersaturated solid solution in these alloys can contain up to 0.77% Si, 0.3% Mg, 4% Cu, which can be very different from the bulk alloy composition (alloy 11 in Table I and alloys 13, 20, 21 and 29 in Table VI). Aging at 170°C of alloy 11 (Table I) results in precipitation of θ', β'' and Si phases on the hardening stage. Upon annealing at 250°C the following phases were observed: θ', β'_C and Si. It is possible that β'_C contained copper and can be designated as the Q phase. However, no chemical analysis of precipitates was performed in this study. Yao *et al*. [55] examined the aging behavior of a similar Al–3.0% Cu–0.39% Mg–7.1% Si alloy at 175°C. They found the θ' phase to be the most pronounced feature of the structure. In addition, needle- and rod-shaped precipitates were observed and tentatively interpreted as β'' and L (β'_C). Other reported results also yield the conclusion that the main hardening phases in silumins are β'' and θ', the appearance of the later depends on the amount of copper in the solid solution [10, 56, 57].

4. Conclusions

The decomposition of supersaturated solid solutions in Al–Cu–Mg–Si alloys may result in the precipitation of several phases, dependent on Mg : Si ratio, copper concentration and annealing temperature. In the range of Mg : Si ratios above the Mg_2Si stoichiometry the phase composition agrees well with that predicted by the equilibrium phase diagram for the temperature of annealing. This suggests that the precipitation paths of the involved phases (Al_2Cu, Mg_2Si, Al_2CuMg) are straightforward from the zone stage to the equilibrium phase through the formation of one or two metastable modifications.

In the solid solutions with an excess of silicon, the precipitation occurs with the formation of Mg_2Si, Al_2Cu, Q (AlMgSiCu) and Si phases. The coherent and semi-coherent modifications of the first two phases act as hardening agents upon aging at temperatures below 200°C. Silicon forms its own particles but does not contribute to hardening. In the hardening stage of precipitation, the coherent β'' and the semicoherent θ' phases are usually observed in Al–Cu–Mg_2Si–Si alloys. Therefore, the equilibrium phase diagram cannot be directly applied to the interpretation of metastable phase composition. In the stage of softening and at temperatures above 200°C, the β'' phase is substituted by semi-coherent β' phases. The unique feature of Al–Mg_2Si–Si alloys is the formation of several semi-coherent modifications of the Mg_2Si (β) phase, different in structure and composition. One of these modifications has the structure identical to that of the equilibrium Q phase and differs from the latter only by composition. Copper, when added to Al–Mg_2Si–Si alloys, may dissolve in coherent and semi-coherent β-based phases. The incorporation of copper atoms in the metastable β-based phases and eventual formation of the equilibrium Q phase in some alloys suggests these β-based phases are precursors of the Q phase. Evidently, the final product of the precipitation path (equilibrium β

or Q) depends on the amount of copper and Mg : Si ratio in the solid solution and on the temperature of annealing. The identity of metastable β'_C and equilibrium Q phases suggests that their crystallographic configuration is thermodynamically efficient. Moreover, the Q phase may be considered as the β' (Mg_2Si-based) phase stabilized by copper, but this requires further investigation.

The sequence of precipitation in Al–Mg_2Si–Si–Cu alloys appears to be as follows:

1. Low copper: s.s.s. – GP zones – β'' (with copper?) – θ' – Si – various modifications of β' (with copper) including β'_C – Mg_2Si, Al_2Cu, Si.
2. High copper: s.s.s. – GP zones – β'' (with copper?) – θ' – Si – various modifications β' (with copper) including β'_C (Q′) – Q (AlMgSiCu), Al_2Cu, Si.
3. At intermediate copper concentrations, in the case of natural aging prior to the artificial aging, and at temperatures above 200°C, the combination of these two precipitation paths may occur.

References

1. A. K. JENA, A. K. GUPTA and M. C. CHATURVEDI, *Metall. Trans.* A **24A** (1993) 2181.
2. D. G. ESKIN, *Z. Metallkde.* **86** (1995) 60.
3. C. R. HUTCHINSON and S. P. RINGER, *Metall. Mater. Trans.* A **31A** (2000) 2721.
4. D. G. ESKIN, *Z. Metallkde.* **83** (1992) 762.
5. D. G. ESKIN, V. MASSARDIER and P. MERLE, *J. Mater. Sci.* **34** (1999) 811.
6. A. CHARAI, T. WALTHER, C. ALFONSO, A.-M. ZAHRA and C. Y. ZAHRA, *Acta Mater.* **48** (2000) 2751.
7. S. HIROSAWA, T. SATO, A. KAMIO and H. M. FLOWER, *ibid.* **48** (2000) 1797.
8. S. P. RINGER and K. HONO, *Mater. Characteriz.* **44** (2000) 101.
9. W. K. ARMITAGE, *J. Inst. Met.* **25** (1970) 46.
10. D. G. ESKIN, V. S. ZOLOTOREVSKII, V. V. ISTOMIN-KASTROVSKII and A. A. AKSENOV, *Russ. Metall.* (2) (1989) 111.
11. V. S. ZOLOTOREVSKII, V. V. ISTOMIN-KASTROVSKII and D. G. ESKIN, *ibid.* (6) (1987) 89.
12. J. M. SILCOCK, T. J. HEAL and H. K. HARDY, *J. Inst. Met.* **82** (1953/1954) 239.
13. L. F. MONDOLFO, "Aluminium Alloys: Structure and Properties" (Butterworths, Boston, 1979).
14. A. A. ALEKSEEV, *Phys. Met. Metallogr.* **75** (1993) 279.
15. K. MATSUDA, Y. SAKAGUCHI, Y. MIYATA, Y. UETANI, T. SATO, A. KAMIO and S. IKENO, *J. Mater. Sci.* **35** (2000) 179.
16. N. MARUYAMA, R. UEMORI, N. HASHIMOTO, M. SAGA and M. KIKUCHI, *Scr. Mater.* **36** (1997) 89.
17. L. ZHEN, W. D. FEI, S. B. KANG and H. W. KIM, *J. Mater. Sci.* **32** (1997) 1895.
18. D. L. ZHANG and D. H. STJOHN, in Proceedings of the International Conference on Aluminum and Magnesium for Automotive Applications, Cleveland, Ohio, 1995 (TMS/AIME, Warrendale, 1996) p. 3.
19. K. MATSUDA, Y. UETANI, T. SATO and S. IKENO, *Metall. Mater. Trans.* A **32A** (2001) 1293.
20. M. MURAYAMA and K. HONO, *Acta Mater.* **47** (1999) 1537.
21. G. A. EDWARDS, K. STILLER, G. L. DUNLOP and M. J. COUPER, *ibid.* **48** (1998) 3893.
22. S. J. ANDERSEN, H. W. ZANDBERGEN, J. JANSEN, C. TRÆHOLT, U. TUNDAL and O. REISO, *ibid.* **46** (1998) 3283.
23. J. P. LYNCH, L. M. BROWN and M. H. JACOBS, *Acta Metall.* **30** (1982) 1389.
24. K. MATSUDA, S. IKENO, T. SATO and A. KAMIO, *Mater. Sci. Forum* **217–222** (1996) 707.
25. K. MATSUDA, S. TADA, S. IKENO and A. KAMIO, in Proceedings of the 4th International Conference on Aluminum Alloys (ICAA'4), Atlanta, 1994, edited by T. H. Sanders, Jr. and A. Starke, Jr. (Georgia Institute of Technology, Atlanta, 1994) p. 598.
26. L. SAGALOWICZ, G. LAPASSET and G. HUG, *Phil. Mag. Lett.* **74** (1996) 57.
27. A. K. GUPTA, D. J. LLOYD and S. A. COURT, *Mater. Sci. Eng.* A **301A** (2001) 140.
28. W. F. MIAO and D. E. LAUGHLIN, *Scr. Mater.* **40** (1999) 873.
29. M. MURAYAMA, K. HONO, W. F. MIAO and D. E. LAUGHLIN, *Metall. Mater. Trans.* A **32A** (2001) 239.
30. G. PHRAGMEN, *J. Inst. Met.* **77** (1950) 489.
31. L. ARNBERG and B. AURIVILLIUS, *Acta Chem. Scand.* A **34** (1980) 1.
32. C. WOLVERTON, *Acta Mater.* **49** (2001) 3129.
33. C. CAYRON, L. SAGALOWICZ, O. BEFFORT and P. A. BUFFAT, *Phil. Mag.* **79** (1999) 2833.
34. C. CAYRON and P. A. BUFFAT, *Acta Mater.* **48** (2000) 2639.
35. V. MASSARDIER, T. EPICIER and P. MERLE, *ibid.* **48** (2000) 2911.
36. I. C. BARLOW, W. M. RAINFORTH and H. JONES, *J. Mater. Sci.* **35** (2000) 1413.
37. R. D. SCHUELLER, F. E. WAWNER and A. K. SACHDEV, *ibid.* **29** (1994) 424.
38. L. M. WANG, H. M. FLOWER and T. C. LINDLEY, *Scr. Mater.* **41** (1999) 391.
39. D. J. CHAKRABARTI, B. CHEONG and D. E. LAUGHLIN, in "Automotive Alloys II," edited by S. K. Das (TMS, Warrendale, 1998) p. 27.
40. N. KH. ABRIKOSOV (Ed.), "Phase Diagrams of Aluminum- and Magnesium-Based Systems" (Nauka, Moscow, 1977).
41. A. PEROVIC, D. D. PEROVIC, G. C. WEATHERLY and D. J. LLOYD, *Scr. Mater.* **41** (1999) 703.
42. G. W. SMITH, W. J. BAXTER and R. K. MISHRA, *J. Mater. Sci.* **35** (2000) 3871.
43. B. DUBOST, J. BOUVAIST and M. REBOUL, in Proceedings of the 1st International Conference on Aluminum Alloys (ICAA'1), Charlottesville, June 1986, Vol. 2 (Engineering Materials Advisory Services Ltd, Warley, 1986) p. 1109.
44. X. GAO, J. F. NIE and B. C. MUDDLE, *Mater. Sci. Forum* **217–222** (1996) 1251.
45. T. SAKURAI and T. ETO, *Kobe Steel and Development* **43**(2) (1993) 95.
46. W. F. MIAO and D. E. LAUGHLIN, *J. Mater. Sci. Lett.* **19** (2000) 201.
47. S. G. BERGSMA, M. E. KASSNER, X. LI and M. A. WALL, *Mater. Sci. Eng.* A **254** (1998) 112.
48. G. C. WEATHERLY, A. PEROVIC, N. K. MUKHOPADHYAY, D. J. LLOYD and D. D. PEROVIC, *Metall. Mater. Trans.* A **32A** (2001) 213.
49. R. K. MISHRA, G. W. SMITH, W. J. BAXTER, A. K. SACHDEV and V. FRANETOVIC, *J. Mater. Sci.* **36** (2001) 461.
50. A. K. GUPTA, M. C. CHATURVEDI and A. K. JENA, *Mater. Sci. Technol.* **5** (1989) 52.
51. S. ABIS, P. MENGUCCI and G. RIONTINO, *Phil. Mag.* **70**(5) (1994) 851.
52. I. DUTTA, C. P. HARPER and G. DUTTA, *Metall. Mater. Trans.* A **25A** (1994) 1591.
53. G. RIONTINO and A. ZANADA, *Mater. Lett.* **37** (1998) 241.
54. W. F. MIAO and D. E. LAUGHLIN, *Metall. Mater. Trans.* A **31A** (2000) 361.
55. J.-Y. YAO, G. A. EDWARDS and D. A. GRAHAM, *Mater. Sci. Forum* **217–222** (1996) 777.
56. R. P. WAHI and M. V. HEIMENDAHL, *Aluminium* **48** (1973) 673.
57. P. OUELLET and F. H. SAMUEL, *J. Mater. Sci.* **34** (1999) 4671.

Received 28 December 2001
and accepted 26 August 2002